Uncertainty quantification and global sensitivity analysis of complex chemical processes with a large number of input parameters using compressive polynomial chaos

Pham Luu Trung Duong[1a], Le Quang Minh[2a], Tram Ngoc Pham[2], Jorge Goncalves[1], Ezra Kwok[3], Moonyong Lee[2†]

[1]Luxembourg Centre for Systems Biomedicine, Systems Control Group, University of Luxembourg, Luxembourg

[2]School of Chemical Engineering, Yeungnam University, Gyeongsan, Rep. of Korea

[3]Chemical & Biological Engineering, University of British Columbia, Vancouver, Canada

(Tel: +82 53-810-2512; Email: mynlee@yu.ac.kr)

[a] These authors contributed equally to this work.

[†]Correspondence concerning this article should be addressed to:

Prof. Moonyong Lee

Email: *mynlee@yu.ac.kr*

Telephone: +82-53-810-2512

[†] Corresponding author.

[a] These authors contributed equally to this work.

ABSTRACT

Uncertainties are ubiquitous and unavoidable in process design and modeling while they can significantly affect safety, reliability, and economic decisions. The large number of uncertainties in complex chemical processes make the well-known Monte-Carlo and polynomial chaos approaches for uncertainty quantification computationally expensive and even infeasible. This study focused on the uncertainty quantification and sensitivity analysis of complex chemical processes with a large number of uncertainties. An efficient method was proposed using a compressed sensing technique to overcome the computational limitations for complex and large scale systems. In the proposed method, compressive sparse polynomial chaos surrogates were constructed and applied to quantify the uncertainties and reflect their propagation effect on process design. Rigorous case studies were provided by the interface between MATLAB™ and Aspen HYSYS™ for a propylene glycol production process and lean dry gas processing plant. The proposed methodology was compared with traditional Monte-Carlo/Quasi Monte-Carlo sampling-based and standard polynomial chaos approaches to highlight its advantages in terms of computational efficiency. The proposed approach could mitigate the simulation costs significantly using an accurate, efficient-to-evaluate polynomial chaos that can be used in place of expensive simulations. In addition, the global sensitivity indices, which show the relative importance of uncertain inputs on the process output, could be derived analytically from the obtained polynomial chaos surrogate model.

Keywords: Generalized polynomial chaos; Uncertainty quantification; Process uncertainty; Sensitivity analysis; Compressed sensing.

1. Introduction

The presence of uncertainty is inevitable in the real-world implementation of engineering systems. The problems of process design under uncertainties have attracted considerable attention, especially regarding safety, reliability, and economic decisions (Abubakar et al., 2015). On the other hand, the design level needs to consider the uncertainty in process inputs, such as pressure, temperature, feed flow, pH, density, concentration, etc. (Arellano-Garcia and Wozny, 2009; Ostrovsky et al., 2012; Sun and Lou, 2008; Vasquez and Whiting, 2004). These uncertainties often have negative influences on the design accuracy. Hence, they need to be accounted for when constructing process models (Beck, 1987). Sensitivity analysis can then be used to identify key parameters that drive the uncertainty of process output predictions qualitatively or quantitatively (Saltelli et al., 2004a).

Most tools available for rigorous process design predict the performance without considering the uncertainties. Hence, it is essential to develop efficient tools for sensitivity analysis (SA) and uncertainty quantification (UQ). The probabilistic approach is a common framework for tracing the effects of uncertainty on the model output. Monte-Carlo (MC) and Quasi Monte-Carlo (QMC) methods are representative probabilistic approaches for the propagation of uncertainties in the model input to its output (Abubakar et al., 2015; Binder, 1998; Caflisch, 1998; Coulibaly and Lécot, 1998; Kroese et al., 2011; Liu, 2008). The principle of MC/QMC methods is to generate an ensemble of random realizations from its uncertainty distribution, to evaluate the model for each element of a sample set, and estimate the relevant statistical properties, such as the mean, standard deviation, and quantile of the output. Despite the simplicity in their implementation, estimations of the mean converge with the inverse square root of the number of runs, making the MC - based approach computationally expensive and even infeasible for most complex chemical process problems. One approach to mitigating the combined simulation cost is to construct an accurate and efficient-to-evaluate surrogate model that can be used in place of expensive simulations (Celse et al., 2015).

Recently, uncertainty analysis using a surrogate model, such as generalized polynomial chaos (gPC) expansion was examined for a range of applications, including modeling, control, robust optimal design, and

fault detection problems. The gPC method, which was first proposed by Wiener (1938), is a spectral representation of a random process by the orthonormal polynomials of random variables. Nagy and Braatz (2007) considered the gPC approach for uncertainty quantification and the robust design for a batch crystallization process. They reported that the gPC approach is more computationally efficient for a system with a moderate number of random inputs than MC/QMC methods. Duong and Lee (2012, 2014) considered the PID controller design for fractional order and integer order systems using the gPC method. Du et al. (2015) examined the fault detection problem by combining the maximum likelihood with the gPC framework. Duong et al. (2016) analyzed the problem of uncertainty quantification/sensitivity analysis of rigorous processes with a small number of random inputs using the standard polynomial chaos (PC) method. Xiu and Karniadakis (2002) further generalized the gPC for non-standard distributions through the Askey scheme.

When adequate smoothness conditions were provided, the gPC expansion for engineering purposes with a uniform and Gaussian distribution showed rapid convergence; in some cases, even exponential convergence was obtained (Ghanem and Spanos, 2003). In theory, there are two main computational schemes for building up a PC model: intrusive and non-intrusive. In the intrusive schemes, the gPC coefficients are obtained by a Galerkin scheme that leads to a system of coupled deterministic equations. Alternatively, a non-intrusive scheme allows the computation of a stochastic model using a set of (decoupled) calls to the existing deterministic model. A current limitation of the standard full non-intrusive gPC approach, where the coefficients are estimated using the tensor cubature, is that the number of model evaluations grows exponentially and may not applicable to systems with a large number of uncertainties. To address this problem, this paper describes a non-intrusive method that builds a sparse gPC expansion using the compressed sensing technique. Under the assumption that the model output prediction produces a sparse representation, the compressed sensing technique can reduce the computational cost compared to the classical full gPC (Blatman and Sudret, 2011). In addition, the limitation of classical full gPC to a system with a large number of uncertainties can be overcome to some extent using the compressed sensing method. Moreover, the Sobol′ sensitivity indices (Sobol′, 2001) can also be obtained directly from the gPC surrogate analytical

model (Crestaux et al., 2009; Haro Sandoval et al., 2012), which can in turn be used to detect the influential inputs in the propagation of process uncertainty.

In this paper, the convergence of an algorithm for UQ and SA is first reported on an analytical function: the Ishigami function. The method is then illustrated using case studies of complex chemical processes, such as a propylene glycol production process and a lean dry gas processing plant. HYSYS^{TM} was used for a rigorous process simulation. The results showed that the proposed compressive gPC-based method could reduce significantly the computational cost (simulation time) for UQ over traditional approaches, such as MC/QMC/gPC methods.

2. Uncertainty quantification using compressive polynomial chaos

Consider a steady-state process described by the following set of nonlinear equations:

$$y = \mathrm{M}(\boldsymbol{\xi}) \tag{1}$$

where $\boldsymbol{\xi} = (\xi_1, \xi_2, ..., \xi_N)$ is a process input variable vector expressed by a random vector of mutually independent random components with probability density functions of $\rho_i(\xi_i): \Gamma_i \to R^+$; and $\mathbf{y}$ denotes a process output (quantity of interest).

The joint probability density of the random vector, $\boldsymbol{\xi}$, is $\boldsymbol{\rho} = \prod_{i=1}^{N} \rho_i$, and the support of $\boldsymbol{\xi}$ is $\boldsymbol{\Gamma} \equiv \prod_{i=1}^{N} \Gamma_i \in R^N$. The uncertainties in the process inputs, $\boldsymbol{\xi}$, are then propagated through the entire process, as shown in Fig.1. The set of one-dimensional orthonormal polynomials, $\{\phi_i(\xi_i)_{m=0}^{d_i}\}$, can be defined in finite dimension space, Γ_i, with respect to the weight, $\rho_i(\xi_i)$. Based on a one-dimensional set of polynomials, an *N*-variate orthonormal set can be constructed with P total degrees in space, $\boldsymbol{\Gamma}$, using the tensor product of the one-dimensional polynomials, the basis function of which satisfies the following:

$$\int_{\boldsymbol{\Gamma}} \Phi_m(\boldsymbol{\xi}) \Phi_n(\boldsymbol{\xi}) \boldsymbol{\rho}(\boldsymbol{\xi}) d\boldsymbol{\xi} = \begin{cases} 1, m = n \\ 0, m \neq n \end{cases}. \tag{2}$$

Consider a process output variable, y, with the statistics (e.g., mean, variance) of interest, the N-variate P^{th} order approximation of the response function can be constructed as follows:

$$\begin{aligned} y_N^P(\boldsymbol{\xi}) &= \sum_{i=1}^{M} f_i \Phi_i(\boldsymbol{\xi}) = \boldsymbol{\mathcal{f}}^T \boldsymbol{\psi}(\boldsymbol{\xi}); \\ M+1 &= \binom{N+P}{N} = \frac{(N+P)!}{N!P!} \end{aligned}, \tag{3}$$

where P is the order of polynomial chaos, and $\boldsymbol{\psi} = \left[\Phi_0(\boldsymbol{\xi}),...,\Phi_M(\boldsymbol{\xi})\right]$ is an assembly of the orthonormal multivariate polynomial, and $\boldsymbol{\mathcal{f}} = \left\{f_1,...,f_M\right\}$ is a vector of the expansion coefficients. The coefficients of gPC expansion can be found by solving the least square minimization problem as follows:

$$\hat{\boldsymbol{\mathcal{f}}} = \arg\min_{\boldsymbol{\mathcal{f}}} \mathbf{E}\left[\left(\boldsymbol{\mathcal{f}}^T \boldsymbol{\psi}(\boldsymbol{\xi}) - \mathrm{M}(\boldsymbol{\xi})\right)^2\right], \tag{4}$$

where $\mathbf{E}[\ ]$ denotes the expectation operator.

For a standard full gPC expansion with the quadrature technique, the solution of Eq. (4) can be approximated as Eq. (A.3). On the other hand, the number of simulations increases exponentially, making it unsuitable for a system with a large number of inputs. In other words, to solve the problem with these large number of inputs, other approaches are used to solve Eq. (4), such as the standard least squares and compressed sensing. These techniques can be explained below.

Given a sample set with the size $Q \approx 2-3M$ of random inputs, $\left\{\boldsymbol{\xi}^{(1)},...,\boldsymbol{\xi}^{(Q)}\right\}$ (experimental design), and the corresponding model outputs, $\mathrm{Y} = \left\{y^{(1)},...,y^{(Q)}\right\}$, the gPC coefficients can be recovered by the least squares method as follows

$$\begin{aligned} \hat{\boldsymbol{\mathcal{f}}}_{ls} &= \arg\min_{\boldsymbol{\mathcal{f}}} \mathbf{E}\left[\left(\boldsymbol{\mathcal{f}}^T \boldsymbol{\psi}(\boldsymbol{\xi}) - \mathrm{M}(\boldsymbol{\xi})\right)^2\right] \\ &\approx \arg\min_{\boldsymbol{\mathcal{f}}} \frac{1}{Q}\sum_{i=1}^{Q}\left[\boldsymbol{\mathcal{f}}^T \boldsymbol{\psi}(\boldsymbol{\xi}^{(i)}) - \mathrm{M}(\boldsymbol{\xi}^{(i)})\right]^2 = \arg\min_{\boldsymbol{\mathcal{f}}} \left\|AF - \mathrm{Y}\right\|_2^2 \end{aligned}, \tag{5}$$

where $\approx$ denotes empirical analogue; $A_{ij} = \Phi_j(\boldsymbol{\xi}^{(i)})$ $i = 1,...,Q$; $j = 1,...,M$ is the experimental matrix. The solution of the least square problem (5) is $\hat{\boldsymbol{\mathcal{f}}}_{ls} = (A^T A)^{-1} A^T \mathrm{Y}$. In this study, the points in the random

experimental design were obtained from the Halton sequence (Kroese et al., 2011; Tempo et al., 2012).

In most engineering applications, only low order interactions between the inputs tend to be important (Doostan and Owhadi, 2011). In other words, the model given in Eq. (1) can be expressed by a sparse expansion in Eq. (3), where most coefficients are zero or negligible. To find the significant polynomials and associated coefficients directly, a selection algorithm, which is known as compressed sensing, can be used.

Under the sparsity assumption, the coefficients of a gPC model can still be recovered effectively with a small sample set with a size $Q < M$ of random inputs and corresponding model outputs as follows:

$$\widehat{\mathcal{F}} = \arg\min_{\mathcal{F}} \mathbf{E}\left[\left(\mathcal{F}^T \boldsymbol{\psi}(\boldsymbol{\xi}) - M(\boldsymbol{\xi})\right)^2\right] + \lambda\|F\|_1 \approx \arg\min_{\mathcal{F}} \|AF - \mathrm{Y}\|_2^2 + \lambda\|F\|_1 \quad (6)$$

where the regularization term, $\lambda\|F\|_1 : \lambda > 0$, forces the minimization to favor the sparse solutions. The optimization problem by Eq. (5) is also known as a l_1 regularized regression. The l_1 regularized regression is a convex optimization that can be solved effectively by many convex optimization techniques, including the alternative direction method of the multiplier (Boyd et al., 2011). There are several reasons why the alternative by Eq. (6) (compressed sensing) might be considered as a least square estimate by Eq. (5) (Hastie et al., 2015), such as

- The prediction accuracy of a least square solution can be improved by shrinking the value of the coefficients or setting some coefficients to zero.
- With a large number of coefficients, the aim would be to identify a smaller subset of these coefficients that are significant.
- The size of the training set (experimental design set) for the compressed sensing method is much smaller than for the standard least square (Q<M).

Let M_A be a surrogate model obtained with the given experimental design; $\mathrm{M}_A^{(-i)}(\boldsymbol{\xi}^{(i)})$ is the surrogate model that has been obtained by the experimental design, $\{\boldsymbol{\xi}^{(1)},...,\boldsymbol{\xi}^{(Q)}\} \setminus \{\boldsymbol{\xi}^{(i)}\}$, i.e., when the i^{th} design point is removed. The leave one out error (prediction accuracy) is defined as

$$Err_{LOO} = \frac{1}{Q}\sum_{i=1}^{Q}\left(\mathrm{M}(\xi^{(i)}) - \mathrm{M}_A^{(-i)}(\xi^{(i)})\right)^2 \tag{7}$$

The leave one out error can be calculated without the need for an explicit calculation of Q in the separate gPC models (Blatman and Sudret, 2011):

$$Err_{LOO} = \frac{1}{Q}\sum_{i=1}^{Q}\left(\frac{\mathrm{M}(\xi^{(i)}) - \mathrm{M}_A(\xi^{(i)})}{1-h_i}\right)^2, \tag{8}$$
$$\left[h_1,...,h_i,...,h_Q\right] = diag(A(A^TA)^{-1}A^T)$$

The regularization coefficient, λ, in Eq. (6) was selected to minimize the leave one out error defined above. Once the vector of the gPC coefficients, $\widehat{\mathcal{F}}=\left\{\widehat{f}_1,...,\widehat{f}_M\right\}$, has been obtained by solving Eq. (6), the statistical properties of the output can be obtained directly as follows. Note that the hat for the coefficients denotes it as an approximation obtained by solving the compressed sensing problem. More detail on compressed sensing techniques can be found elsewhere (Foucart and Rauhut, 2013; Hastie et al., 2015) and the references therein.

The mean value of the output can be expressed as

$$\mathbf{E}[y] = \mu_y = \int_\Gamma y_N^P \rho(\xi) d\xi = \int_\Gamma \left[\sum_{j=1}^{M}\widehat{f}_j\Phi_j(\xi)\right]\rho(\xi)d\xi = \widehat{f}_1. \tag{9}$$

The variance of the output can be evaluated as follows:

$$D_y = \sigma^2{}_y = \mathbf{E}[(y-\mu_y)^2] = \int_\Gamma (\sum_{j=1}^{M}\widehat{f}_j(\xi)\Phi_j(\xi) - \widehat{f}_1)(\sum_{j=1}^{M}\widehat{f}_j(\xi)\Phi_j(\xi) - \widehat{f}_1)\rho(\xi)d\xi = \sum_{j=2}^{M}\widehat{f}_j{}^2 .$$

(10)

The distribution function of the output is obtained by sampling the surrogate model in Eq. (3).

Remarks: An input ξ_i is distributed according to the density $\rho_i(\xi_i)$, and $\{\phi_i(\xi_i)\}$ are polynomials that are orthonormal with respect to $\rho_i(\xi_i)$. For several commonly used distributions, such an association between $\rho_i(\xi_i)$ and $\{\phi_i(\xi_i)\}$ is given by the Askey scheme. For a general distribution, the methods in Gautschi (2004) and the references therein can be used to construct an associated set of polynomials. The gPC coefficients

can also be calculated by numerical integration with a cubature, which will be referred as a full (non -intrusive) gPC expansion. Note that the number of simulations required using a full gPC expansion increases exponentially, leading to a significant computational burden. More details on full (non -intrusive) gPC expansion and Askey scheme are given in Appendix A.

3. Variance based-sensitivity analysis using compressive gPC

To separate the single and collective contribution of each input, the gPC expansions in Eq. (3) can be reordered as follows.

Define the set of multi-indices $I_{k_1,\ldots,k_s}$ such that (Haro Sandoval et al., 2012):

$$I_{k_1,\ldots,k_s} = \left\{(k_1 k_2,\ldots,k_s) : 0 \le \mathrm{g}_k^j \le P, \mathrm{g}_k^j = 0, k \in \{1,\ldots,n\} \setminus \{k_1,\ldots,k_s\}\right\} \tag{11}$$

where g_k^j is the one-dimensional polynomial degree. Using this notation, the first order sensitivity function can be expressed as

$$S_i = \frac{\sum_{j \in I_i} \widehat{f}_j^{\,2}}{D_f}. \tag{12}$$

The estimated sensitivity function of a higher order can be obtained in the same manner as follows:

$$S_{i_1,\ldots,i_s} = \frac{\sum_{j \in I_{i_1,\ldots,i_s}} \widehat{f}_j^{\,2}}{D_f}. \tag{13}$$

The total sensitivity functions, T_i, can be obtained by summing all the sensitivity functions involving the input ξ_i. This quantifies the total impact of an input ξ_i, including all the interactions with the other inputs.

4. Examples

In this section, the proposed compressive gPC-based method was applied to the uncertainty quantification and sensitivity analysis of an analytical example and two complex chemical process examples. This study

aims to explain the practical, accurate, and efficient-to-evaluate procedure involving SA and UQ.

4.1. **Example 1:** Ishigami functions

The Ishigami function, which is a well-known example in uncertainty quantification and sensitivity analysis, was considered to demonstrate the accuracy of compressive polynomial chaos:

$$y = \sin(\xi_1) + a\sin^2(\xi_2) + b\xi_3^4 \sin(\xi_1)\ , \tag{14}$$

with $\xi_i \quad i = 1,..3$ distributed uniformly in $[-\pi\ \pi]$. The total variance D_y and partial variance $D_j,...$ can be computed analytically as

$$\begin{aligned} D_y &= \frac{a^2}{8} + \frac{b\pi^4}{5} + \frac{b^2\pi^8}{18} + \frac{1}{2} \\ D_1 &= \frac{b\pi^4}{5} + \frac{b^2\pi^8}{50} + \frac{1}{2} \\ D_2 &= \frac{a^2}{8} \quad D_{13} = \frac{b^2\pi^8}{18} - \frac{b^2\pi^8}{18} \\ D_3 &= D_{12} = D_{23} = D_{123} = 0 \end{aligned} \tag{15}$$

For a numerical study, $a = 7,\ b = 0.1$. The true value of the sensitivity indices can be obtained easily from Eq. (23). Owing to the very high non-linearity of the Ishigami function, a relatively high polynomial degree of $P = 14$ is needed to achieve a satisfactory result for a full gPC and compressive gPC. Table 1 lists the results of compressive gPC along with those of full gPC and QMC (with Halton sequence). The convergence rate of the QMC method was quite slow compared to the other two methods and it had a negative value for S_3, which is a non-negative quantity by definition. The compressive gPC approach can provide a similar result to the full gPC expansion with considerably fewer simulations. Fig.2 presents the density function of the Ishigami function with 10000 QMC simulations and the density function from sampling the compressive and full gPC models. The density function by the three methods matched well with each other. Note that for uncertainty quantification purposes, only 250 simulations were sufficient to construct the compressive gPC model that can predict the density function of the Ishigami function accurately, whereas the full gPC model with a similar number of simulations (343 runs) showed an apparent deviation from the true density function, as shown in Fig.2.

4.2. Example 2: propylene glycol production process with six uniform uncertainties in process inputs

Referring the conceptual model from HYSYS^{TM}, Fig. 3 presents a flow diagram of a propylene glycol (PG) production process. In this process, propylene oxide (PO) is reacted with water to produce PG in a continuously-stirred-tank reactor (CSTR). Because the reaction is exothermic, a coolant fluid circulates within the reactor jacket to maintain its temperature. The reactor outlet stream is then fed to a distillation column, where essentially all the glycol product is recovered from the column bottom with 99.5 wt. % of PG. The distillation column has 10 stages with a full reflux condenser and reboiler operating at atmospheric pressure.

In this example, the flow rates of PO and water, the temperature and pressure of the mixed stream, the temperature of the reactor effluent, and the reflux ratio of the column were assumed to be independently uncertain and distributed uniformly in intervals of

$\{$[61.2; 74.8 kgmol/h], [249.3; 304.7 kgmol/h], [21.5; 26.3 ^{o}C], [1.1; 1.3 bars], [57; 63 ^{o}C], [0.9; 1.1]$\}$, respectively.

A simulation set of 1000 samples from the QMC sequence was generated using the MATLAB^{TM} code Halton set and was passed to HYSYS^{TM}, where the PG process in Fig.3 was modeled rigorously. The outputs from HYSYS^{TM} were collected and used for the compressive sensing problem in Eq. (5) to recover the gPC coefficients of the gPC model with a total order of 12. The order of gPC was chosen to be the lowest so that the gPC model can reflect the non-linearity of the distillation column. The size $Q = 1000$ was chosen for the experimental design set based on the heuristic studies and guidelines from Doostan and Owhadi (2011). Note that the full gPC expansion requires 10^6 simulations, which leads to an excessive increase in the computational time (approximately 1000 times slower than the proposed method). Because the true estimates of the output for the process studied are unavailable, the results from the proposed method were compared with those from the QMC method with a sufficiently large number of samples. The number of samples for the QMC method can be chosen according to the Chernoff bound (Tempo et al., 2012) for an accurate estimation of the probability. Table 2 lists the statistical properties of the reboiler duty (Q) obtained from the compressive gPC method (proposed) and the conventional QMC methods. Fig.4 compares the density

functions of the reboiler duty obtained from the compressive gPC/ QMC methods. The results from the proposed gPC method matched those from the traditional QMC method. Table 2 also lists the computational time required for both methods. The computational time for the proposed method includes the computational time for both solving the compressed sensing problem and performing the simulations from the experimental design.

The gPC coefficients can be used to calculate the Sobol′ sensitivity indices, which can identify the influential inputs in the propagation of process uncertainty, as well as further reduce the number of simulations and the computational efforts needed for the uncertainty quantification up to 10-100 times. Table 3 lists the sensitivity indices obtained from the gPC model. The results showed that the water flow rate and the reflux ratio are two inputs that matter. In other words, the propylene oxide flow rate, the temperature and pressure of the mixed stream, and the outlet temperature of the reactor effluent are non-influential and can be excluded from the analysis of uncertainty propagation. Therefore, owing to the effective detection of non-influential input of compressive gPC, one can simplify the model, and the standard gPC approach with cubature, which requires only 49 simulations, can be used for UQ instead of the compressive gPC. On the other hand, for the QMC, the same number of simulations are still needed to obtain a reliable prediction of the uncertainty. Fig. 5 compares the density distributions predicted using the standard gPC and QMC methods with two influential random inputs (i.e., the water flow rate and the reflux ratio) and that by the QMC method (with 10000 simulations from Halton sequence) with all six random inputs.

4.3. **Example 3**: lean dry gas processing plant with six uniform uncertainties

Fig. 6 shows a process flow diagram of a lean dry gas production process (AspenHYSYS, 2006). A natural gas stream containing N_2, CO_2, and C_1 - n-C_4 is processed in a refrigerated system to remove the heavier components. The combined feed stream enters an inlet separator, which removes the free liquids. The overhead gas from the separator is fed to the gas/gas exchanger, where it is pre-cooled by an already refrigerated gas. The cooled gas is then fed to the cooler, where further cooling is accomplished. In the cooler, a sufficient quantity of heavier hydrocarbons condense such that the eventual sales gas meets the dew point

281 requirements of the pipeline for that particular hydrocarbon. The cold stream is then separated in a low-
282 temperature separator. The cold dry gas is fed to the gas/gas exchanger and is then sent for sale, whereas the
283 condensed liquids are mixed with the free liquids from the inlet separator. In this process, the lean dry gas
284 produced will meet the hydrocarbon dew point requirements, and heat duty specifications, etc. Furthermore,
285 the liquid stream coming from the mixer is fed to a depropanizer column to produce a low-propane-content
286 bottom product. In this example, the sale gas heating value is controlled while the flow rates (*F1* and *F2*),
287 temperature (*Tn*) and pressure (*Pn*) of two natural gas inlets, the outlet temperature of the cooled gas (*Tc*),
288 and the reflux ratio in the distillation column (*R*) are assumed to have uncertainties with a uniform distribution
289 in the range, $F1 \in [1.90; 2.32$ kg/s], $F2 \in [1.25; 1.52$ kg/s], $Tn \in [14.0; 17.1$ °C], $Pn \in [37.2; 45.5$ bars],
290 $Tc \in [-16.8; -13.8$ °C] and $R \in [0.9; 1.1]$.

291 Fig. 7 shows the density functions for the net heating value of sale gas using the compressive gPC/ QMC
292 methods. The results from the compressive gPC method (10^{th} order gPC with 1000 simulations) closely
293 matched those from the QMC methods with 10000 simulations. Table 2 lists the statistical properties of the
294 lean gas heating value and simulation parameters from the proposed gPC and QMC methods. In addition,
295 Table 3 lists the sensitivity indices obtained from the surrogate gPC model. The sensitivity indices indicate
296 that the pressure of the NG inlet and the outlet temperature of the cooled gas affect the uncertainty
297 propagation while other parameters can be fixed. Again, the standard gPC approach can be used for UQ with
298 only 2 random inputs. Fig. 8 shows the density functions of lean gas production with two influential random
299 inputs using the standard gPC method (with 100 simulations) and by the QMC method (with 10000
300 simulations); the result compares well with that of the QMC method using all six random parameters with
301 10000 simulations. As a result, the sensitivity indices from the compressive gPC method can identify the
302 influential inputs correctly. The order and size of the experimental design were selected to be the same as
303 those in the previous example.

Remark Owing to the exponential increase in simulation efforts for cases with six random inputs, the standard gPC method was not considered for UQ in Examples 2 and 3. In addition, the QMC method was not used for SA in Examples 2 and 3 because of the requirement of huge computational effort for SA using the QMC method (This will be approximately 8 times more than the effort for UQ). For more details on SA with the QMC method, please see Appendices B and C.

5. Conclusions

Sensitivity analysis and uncertainty quantification can be useful for a range of purposes, such as

- Testing the robustness of a process model in the presence of uncertainty,
- Increasing the understanding of the relationships between the input and output of a process model,
- Achieving model simplification by fixing the uncertain inputs that have little effect on the output.

To tackle the practical and time-consuming problems of uncertainty propagation and sensitivity analysis, a sparse polynomial chaos method with compressed sensing was proposed for complex chemical processes with a moderate/large number of uncertain parameters. In most engineering applications, only low order interactions between the parameters tend to be important: a process model (1) can be expressed by a sparse expansion in terms of polynomial chaos. The compressed sensing technique allows sparse polynomial chaos to be recovered from a small number of sampling points. HYSYS^{TM} was used to obtain a rigorous result in all simulations. The results showed precise agreement with those of the conventional approaches, such as the QMC/ standard gPC methods, which might be beyond the computational capability for large scale complex chemical process problems with a moderate/large number of uncertainties. The compressive gPC approach has advantages over the popular QMC/gPC approaches, mainly in terms of the computational cost when a large number of random inputs are considered. Sobol′ sensitivity indices, which can be used to detect non-influential inputs, simplified the models for UQ of the propylene glycol production process and the lean dry gas processing plant.

ACKNOWLEDGMENTS

This study was supported by the Basic Science Research Program through the National Research Foundation of Korea (NRF) funded by the Ministry of Education (2015R1D1A3A01015621), and also by the Priority Research Centers Program through the National Research Foundation of Korea (NRF) funded by the Ministry of Education (2014R1A6A1031189). Pham L.T. Duong and Jorge Goncalves were supported by FNR CORE project ref 8231540. The authors would like to thank Dr. Ye Yuan and Junyang Jin for useful discussion on the compressed sensing technique.

APPENDIX A: Full gPC expansion with numerical integration and Askey scheme

Normally when a full gPC expansion is considered, all gPC coefficients in Eq. (3) are obtained from the multidimensional integral,

$$f_i = \mathbf{E}[\Phi_i M(\boldsymbol{\xi})] = \int_{\Gamma} M(\boldsymbol{\xi})\Phi_i(\boldsymbol{\xi})\rho(\boldsymbol{\xi})d\boldsymbol{\xi}. \quad \text{(A.1).}$$

In the discrete projection approach, Eq. (A.1) can be computed numerically using the following procedure (Xiu and Karniadakis, 2002):

- Choose an N-dimensional integration rule with $q_1 \times \ldots \times q_N$ cubature nodes/weights,

$$\ell^{q_1 \times \ldots \times q_N}[g] = \sum_{j_1=1}^{q_1} \ldots \sum_{j_N=1}^{q_N} g(\xi_1^{(j_1)}, \ldots, \xi_N^{(j_n)})(w_1^{(j_1)} \ldots w_N^{(j_N)}) \simeq \int_{\Gamma} g(\boldsymbol{\xi})\rho(\boldsymbol{\xi})d\boldsymbol{\xi}, \quad \text{(A.2)}$$

where $\ell^{q_1 \times \ldots \times q_N}[\cdot]$ denotes the multivariate cubature approximation. Normally, the Gaussian tensorized cubature is used.

- Approximate the gPC coefficients in Eq. (A.1) using the numerical integration rule in Eq. (A.2).

$$\tilde{\tilde{f}}_j = \ell^{q_1 \times \ldots \times q_N}[\mathrm{M}(\boldsymbol{\xi})\Phi(\boldsymbol{\xi})\boldsymbol{\rho}] = \sum_{m=1}^{q_1 \times \ldots \times q_N} \mathrm{M}(\boldsymbol{\xi}^{(m)})\Phi_j(\boldsymbol{\xi}^{(m)})w^{(m)} \quad , \quad \text{(A.3)}$$

where $\tilde{\tilde{f}}_j$ is approximated numerically by the cubature. $\mathrm{M}(\boldsymbol{\xi})\Phi_j(\boldsymbol{\xi})$ plays a role of $g(\boldsymbol{\xi})$ in Eq. (A.2). The number of nodes (simulations) in the cubature rule increases exponentially.

The set of polynomials is orthonormal with the weight function, which is the probability density function. The Askey scheme below links the distributions of a random variable and the type of classical orthonormal gPC basis.

Table A1. Orthogonal polynomial corresponding to several commonly used continuous distributions from the Askey scheme

Type of random input	Polynomial chaos	Weight (density function) and Support
Gaussian	Hermite	$\rho_i(\xi_i)=\frac{1}{\sqrt{2\pi}}e^{-\xi_i^2/2}$ $\Gamma_i=(-\infty,\infty)$
Beta	Jacobi	$\rho_i(\xi_i)=\frac{\Gamma(\alpha+\beta+2)}{2^{\alpha+\beta+1}\Gamma(\alpha+1)\Gamma(\beta+1)}(1-\xi_i)^{\alpha}(1+\xi_i)^{\beta}$ $\Gamma_i=[-1,1]$
Gamma	Laguerre	$\rho_i(\xi_i)=\xi_i^{\alpha}e^{-\xi_i}/\Gamma(\alpha+1)$ $\Gamma_i=(0,\infty)$

Note that Legendre polynomials are a special case of the Jacobi polynomial with parameter $\alpha=\beta=0$. The first three Legendre polynomials (for uniform input) are

$\phi_0(\xi_i)=1,\quad \phi_1(\xi_i)=1.7321\xi_i,\quad \phi_2(\xi_i)=3.3541\xi_i^2-1.1180$.

APPENDIX B: Brief theory of variance-based sensitivity analysis

Consider the system described in Fig.1 and Eq. (1). The mean and variance of the output are defined as

$$\mu_y=\int_{\Gamma_1}\cdots\int_{\Gamma_N} y(\xi_1,\ldots,\xi_N)\prod_{i=1}^{N}\rho_i(\xi_i)d\xi_i \tag{B.1}$$

$$D_y=\int_{\Gamma_1}\cdots\int_{\Gamma_N}\left[(y(\xi_1,\ldots,\xi_N))-\mu_y\right]^2\prod_{i=1}^{N}\rho_i(\xi_i)d\xi_i .$$

The system output can be decomposed into a sum of terms with increasing dimensions as follows: (Saltelli et al., 2008; Saltelli et al., 2004a, b):

$$y(\boldsymbol{\xi}) = y_0 + \sum_{i=1}^{N} y_i(\xi_i) + \sum_{i=1}^{N-1}\sum_{j>i}^{N} y_{ij}(\xi_i,\xi_j) + \ldots + y_{i_1\ldots i_N}(\xi_i,\ldots,\xi_N) \tag{B.2}$$

where $y_0 = \mu_y$.

The terms in Eq. (12) can be expressed as

$$\begin{aligned} y_i(\xi_i) &= \mathbf{E}\left[\mathrm{y}(\boldsymbol{\xi})\middle|\xi_i\right] - \mu_y \\ y_{ij}(\xi_i,\xi_j) &= \mathbf{E}\left[\mathrm{y}(\boldsymbol{\xi})\middle|\xi_i,\xi_j\right] - y_i - y_j - \mu_y \\ &\ldots \end{aligned} \tag{B.3}$$

where $\mathbf{E}\left[\mathrm{y}(\boldsymbol{\xi})\middle|\xi_i\right]$ (resp. $\mathbf{E}\left[\mathrm{y}(\boldsymbol{\xi})\middle|\xi_i,\xi_j\right]$) is the conditional expectation of $y(\boldsymbol{\xi})$ when ξ_i is set (resp. ξ_i and ξ_j are set).

Provided that the random input factors are independent, the decomposition in Eqs. (B.2) and (B.3) is unique. By taking the variance of both sides of Eq. (B.2), the variance of the output function can be decomposed as follows:

$$D_y = \sum_{i=1}^{N} D_i + \sum_{i=1}^{N-1}\sum_{j>i}^{N} D_{ij} + \ldots + D_{1,2,\ldots,N}, \tag{B.4}$$

where

$$\begin{aligned} D_i &= \mathrm{var}\left(\mathbf{E}\left[y(\boldsymbol{\xi})\middle|\xi_i\right]\right) \\ D_{ij} &= \mathrm{var}\left(\mathbf{E}\left[y(\boldsymbol{\xi})\middle|\xi_i,\xi_j\right]\right) - D_i - D_j \\ &\ldots \\ D_{1,2,\ldots,N} &= D_{f_y} - \sum_{i=1}^{N} D_i - \ldots - \sum_{1\le i_1<\cdots<i_{n-1}\le N} D_{i_1\ldots i_{N-1}} \end{aligned} \tag{B.5}$$

Note that in $\mathrm{var}\left(\mathbf{E}\left[f(y(\boldsymbol{\xi}))\middle|\xi_i,\xi_j\right]\right)$, the inner expectation is greater than all the factors except for ξ_i,ξ_j, and the outer variance is greater then ξ_i,ξ_j.

The first order Sobol′ sensitivity index (function) can be defined as

$$S_i = \frac{D_i}{D_{f_y}}. \tag{B.6}$$

The first order index, S_i, measures the amount of the output variance that is explained by the parameter, ξ_i, alone. S_i lies in [0,1]. The sum of the first order indices will equal 1 for the additive models.

Similarly, define the sensitivity functions of a higher order, a sensitivity measure that describes what part of the total variance is due to uncertainties in the set of inputs, $\{\xi_{i_1},...,\xi_{i_s}\}$, as

$$S_{i_1,...,i_k} = \frac{D_{i_1,...,i_k}}{D_{f_y}}. \tag{B.7}$$

The Sobol′ total effect function for the factor, ξ_i, can be expressed as

$$T_i = 1 - \frac{\mathrm{var}(\mathbf{E}(f_y(\boldsymbol{\xi})\,|\,\boldsymbol{\xi}_{\sim i}))}{D_{f_y}(t)}. \tag{B.8}$$

This total effect index measures the contribution to the output variance of ξ_i, including all the variances caused by its interactions, of any order, with any other parameters. In other words, if T_i is close to zero, the ith parameter, ξ_i, can be neglected.

APPENDIX C: Estimation of Sobol′ indices by the MC/QMC methods

This section briefly describes the MC method for estimating the Sobol′ indices (Saltelli et al., 2008; Saltelli et al., 2004b).

- Generate a $\mathrm{A}_{Q\times N}$ matrix (Q is the size of sample) from a given density function of inputs.

$$\mathrm{A}_{Q\times N} = \begin{bmatrix} \xi_1^{(1)} & \cdots & \xi_i^{(1)} & \cdots & \xi_N^{(1)} \\ \cdots & \cdots & \cdots & \cdots & \cdots \\ \xi_1^{(Q)} & \cdots & \xi_i^{(Q)} & \cdots & \xi_N^{(Q)} \end{bmatrix}. \tag{C.1}$$

- Generate a $\mathrm{B}_{Q\times N}$ matrix (independent from A) from the given density function of inputs.

$$\mathrm{B}_{Q\times N} = \begin{bmatrix} \xi_1^{(Q+1)} & \cdots & \xi_i^{(Q+1)} & \cdots & \xi_N^{(Q+1)} \\ \cdots & \cdots & \cdots & \cdots & \cdots \\ \xi_1^{(2Q)} & \cdots & \xi_i^{(2Q)} & \cdots & \xi_N^{(2Q)} \end{bmatrix}. \tag{C.2}$$

- Define a matrix, C_i, which is formed by all columns of B except the i^{th} column, which is taken from A.
- Compute the output of the model (1) for all input values in the sample matrices $\mathrm{A}, \mathrm{B}, \mathrm{C}_i$, obtaining vectors of model output $y_{\mathrm{A}} = M(\mathrm{A})$, $y_{\mathrm{B}} = M(\mathrm{B})$, $y_{\mathrm{C}_i} = M(\mathrm{C}_i)$.
- The first order indices are estimated as follows:

$$S_i = \frac{(1/Q)\sum_{j=1}^{Q} y_{\mathrm{A}}^{(j)} y_{\mathrm{C}_i}^{(j)} - M_0^{\,2}}{(1/Q)\sum_{j=1}^{Q} (y_{\mathrm{A}}^{(j)})^2 - M_0^{\,2}}, \tag{C.3}$$

where $M_0^2 = \left((1/Q)\sum_{i=1}^{Q} y_{\mathrm{A}}^{(j)} \right)^2$ is the empirical mean of the model output.

The total order indices are estimated as follows:

$$T_i = 1 - \frac{(1/Q)\sum_{j=1}^{Q} y_{\mathrm{B}}^{(j)} y_{\mathrm{C}_i}^{(j)} - M_0^{\,2}}{(1/Q)\sum_{j=1}^{Q} (y_{\mathrm{A}}^{(j)})^2 - M_0^{\,2}}. \tag{C.4}$$

Because there are *N* inputs, the cost of this approach is 2*Q* runs of the model for matrices A, B plus N times *Q* for matrices C_i. Hence, the total computational cost is *Q(N+2)*.

REFERENCES

[1] Abubakar, U., Sriramula, S., Renton, N.C., 2015. Reliability of complex chemical engineering processes. Comput. Chem. Eng. 74, 1-14.

[2] Arellano-Garcia, H., Wozny, G., 2009. Chance constrained optimization of process systems under uncertainty: I. Strict monotonicity. Comput. Chem. Eng. 33, 1568-1583.

[3] AspenHYSYS, 2006. Aspentech. [accessed on 30.04.16] http://www.aspentech.com/core/aspen-hysys.aspx.

[4] Beck, M.B., 1987. Water quality modeling: A review of the analysis of uncertainty. Water Resour. Res. 23, 1393-1442.

[5] Binder, K., 1998. Monte Carlo Methods: a powerful tool of statistical physics, Springer, New York, pp. 19-39.

[6] Blatman, G., Sudret, B., 2011. Adaptive sparse polynomial chaos expansion based on least angle regression. J. Comput. Phys. 230, 2345-2367.

[7] Boyd, S., Parikh, N., Chu, E., Peleato, B., Eckstein, J., 2011. Distributed Optimization and Statistical Learning via the Alternating Direction Method of Multipliers. Found. Trends Mach. Learn. 3, 1-122.

[8] Caflisch, R.E., 1998. Monte Carlo and quasi-Monte Carlo methods. Acta Numerica 7, 1-49.

[9] Celse, B., Costa, V., Wahl, F., Verstraete, J.J., 2015. Dealing with uncertainties: Sensitivity analysis of vacuum gas oil hydrotreatment. Chem. Eng. J. 278, 469-478.

[10] Coulibaly, I., Lécot, C., 1998. Monte Carlo and quasi-Monte Carlo algorithms for a linear integro-differential equation, Springer, New York, pp. 176-188.

[11] Crestaux, T., Le Maıˆtre, O., Martinez, J.-M., 2009. Polynomial chaos expansion for sensitivity analysis. Reliab. Eng. Syst. Saf. 94, 1161-1172.

[12] Doostan, A., Owhadi, H., 2011. A non-adapted sparse approximation of PDEs with stochastic inputs. J. Comput. Phys. 230, 3015-3034.

[13] Du, Y., Duever, T.A., Budman, H., 2015. Fault detection and diagnosis with parametric uncertainty using generalized polynomial chaos. Comput. Chem. Eng. 76, 63-75.

[14] Duong, P.L.T., Lee, M., 2012. Robust PID controller design for processes with stochastic parametric uncertainties. J. Process Control 22, 1559-1566.

[15] Duong, P.L.T., Lee, M., 2014. Probabilistic analysis and control of systems with uncertain parameters over non-hypercube domain. J. Process Control 24, 358-367.

[16] Duong, P.L.T., Wahid, A., Kwok, E., Lee, M., 2016. Uncertainty quantification and global sensitivity analysis of complex chemical process using a generalized polynomial chaos approach. Comput. Chem. Eng.90, 23-30.

[17] Foucart, S., Rauhut, H., 2013. A Mathematical Introduction to Compressive Sensing. Birkhäuser Basel.

[18] Gautschi, W., 2004. Orthogonal Polynomials: Computation and Approximation. Oxford University Press.

[19] Ghanem, R.G., Spanos, P.D., 2003. Stochastic finite elements: a spectral approach. Dover Publications, New York.

[20] Haro Sandoval, E., Anstett-Collin, F., Basset, M., 2012. Sensitivity study of dynamic systems using polynomial chaos. Reliab. Eng. Syst. Saf. 104, 15-26.

[21] Hastie, T., Tibshirani, R., Wainwright, M., 2015. Statistical Learning with Sparsity: The Lasso and Generalizations. Taylor & Francis.

[22] Kroese, D.P., Taimre, T., Botev, Z.I., 2011. Markov Chain Monte Carlo, Handbook of Monte Carlo Methods. John Wiley & Sons, Inc., pp. 225-280.

[23] Liu, J.S., 2008. Monte Carlo Strategies in Scientific Computing. Springer-Verlag, New York.

[24] Nagy, Z.K., Braatz, R.D., 2007. Distributional uncertainty analysis using power series and polynomial chaos expansions. J. Process Control 17, 229-240.

[25] Ostrovsky, G.M., Ziyatdinov, N.N., Lapteva, T.V., Zaitsev, I.V., 2012. Optimization of chemical processes with dependent uncertain parameters. Chem. Eng. Sci. 83, 119-127.

[26] Saltelli, A., Ratto, M., Andres, T., Campolongo, F., Cariboni, J., Gatelli, D., Saisana, M., Tarantola, S., 2008. Global sensitivity analysis: the primer. John Wiley & Sons.

[27] Saltelli, A., Tarantola, S., Campolongo, F., Ratto, M., 2004a. Global Sensitivity Analysis for Importance Assessment, Sensitivity Analysis in Practice. John Wiley & Sons, Ltd, pp. 31-61.

[28] Saltelli, A., Tarantola, S., Campolongo, F., Ratto, M., 2004b. Methods Based on Decomposing the Variance of the Output, Sensitivity Analysis in Practice. John Wiley & Sons, Ltd, pp. 109-149.

[29] Sobol′, I.M., 2001. Global sensitivity indices for nonlinear mathematical models and their Monte Carlo estimates. Math. Comput. Simulation 55, 271-280.

[30] Sun, L., Lou, H.H., 2008. A strategy for multi-objective optimization under uncertainty in chemical process design. Chinese J. Chem. Eng. 16, 39-42.

[31] Tempo, R., Calafiore, G., Dabbene, F., 2012. Randomized algorithms for analysis and control of uncertain systems: with applications. Springer Science & Business Media.

[32] Vasquez, V.R., Whiting, W.B., 2004. Analysis of random and systematic error effects on uncertainty propagation in process design and simulation using distribution tail characterization. Chem. Eng. Commun. 191, 278-301.

[33] Wiener, N., 1938. The homogeneous chaos. Am. J. Math. 60, 897-936.

[34] Xiu, D., Karniadakis, G.E., 2002. The Wiener--Askey Polynomial Chaos for Stochastic Differential Equations. SIAM J. Sci. Comput. 24, 619-644.

List of Figures

Fig. 1. Uncertainty propagation and quantification in chemical processes.

Fig. 2. Density function of the Ishigami function (Example 1).

Fig. 3. Propylene glycol (PG) production process.

Fig. 4. Density distributions of the reboiler duty in the PG production process with 6 uniform random inputs (Example 2).

Fig. 5. Density distributions of the reboiler duty in the PG production process with 6 and 2 uniform random inputs (Example 2).

Fig. 6. Lean dry gas processing plant (Example 3).

Fig. 7. Density distributions of the net heating value of sale gas in the lean dry gas production process with 6 uniform random inputs (Example 3).

Fig. 8. Density distributions of the net heating value of sale gas in the lean dry gas production process (Example 3) with 6 and 2 uniform random inputs.

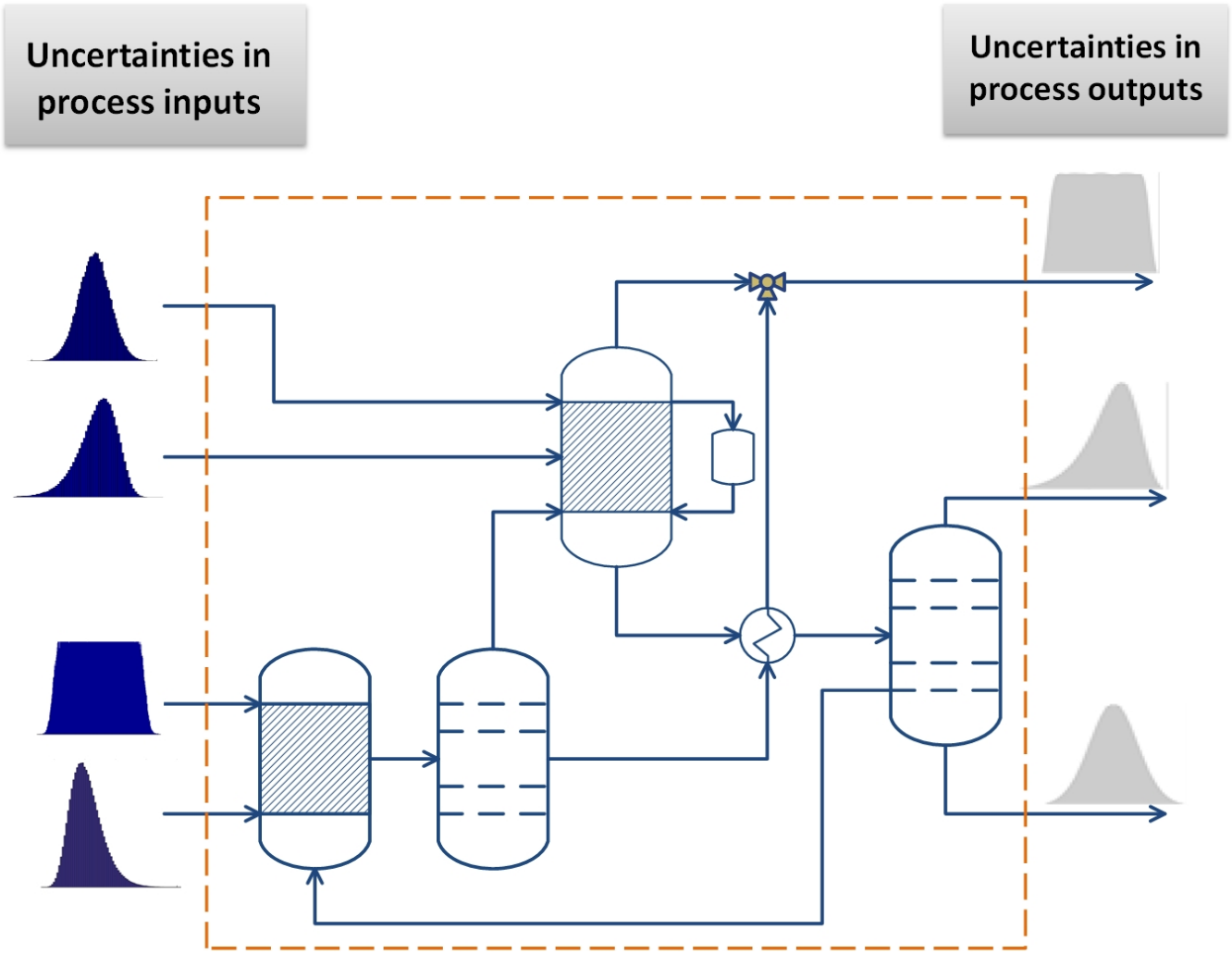

Fig. 1. Uncertainty propagation and quantification in chemical processes.

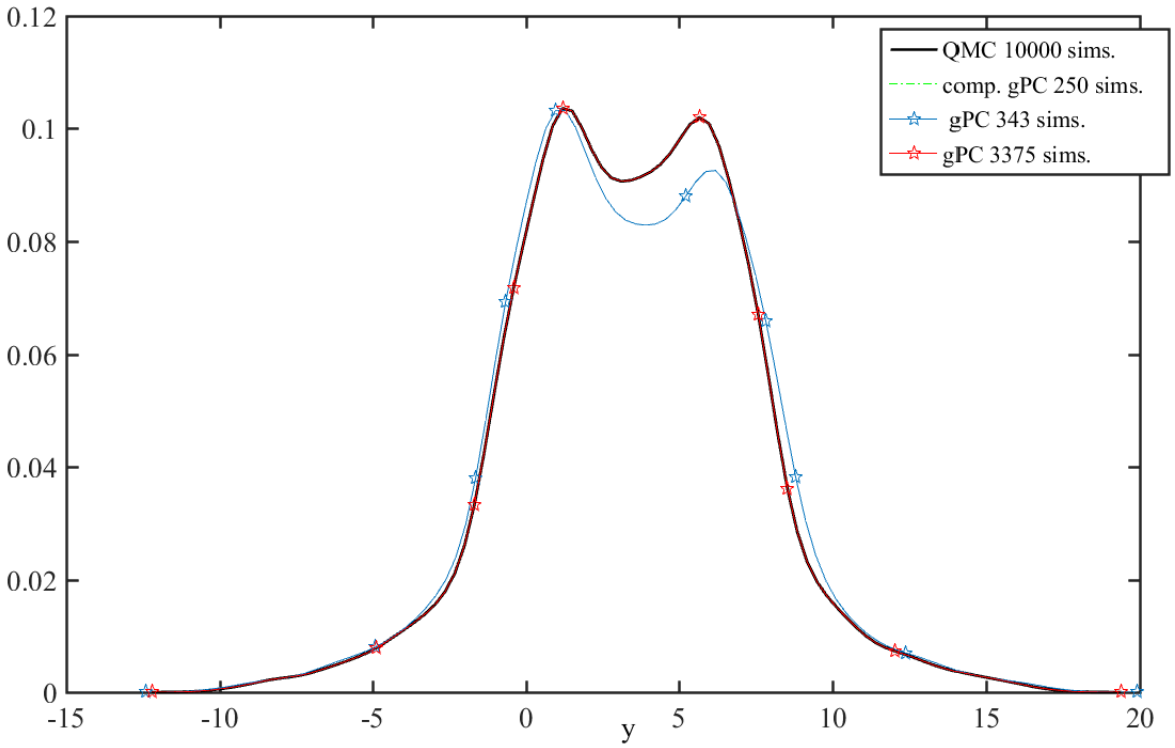

Fig. 2. Density function of the Ishigami function (Example 1).

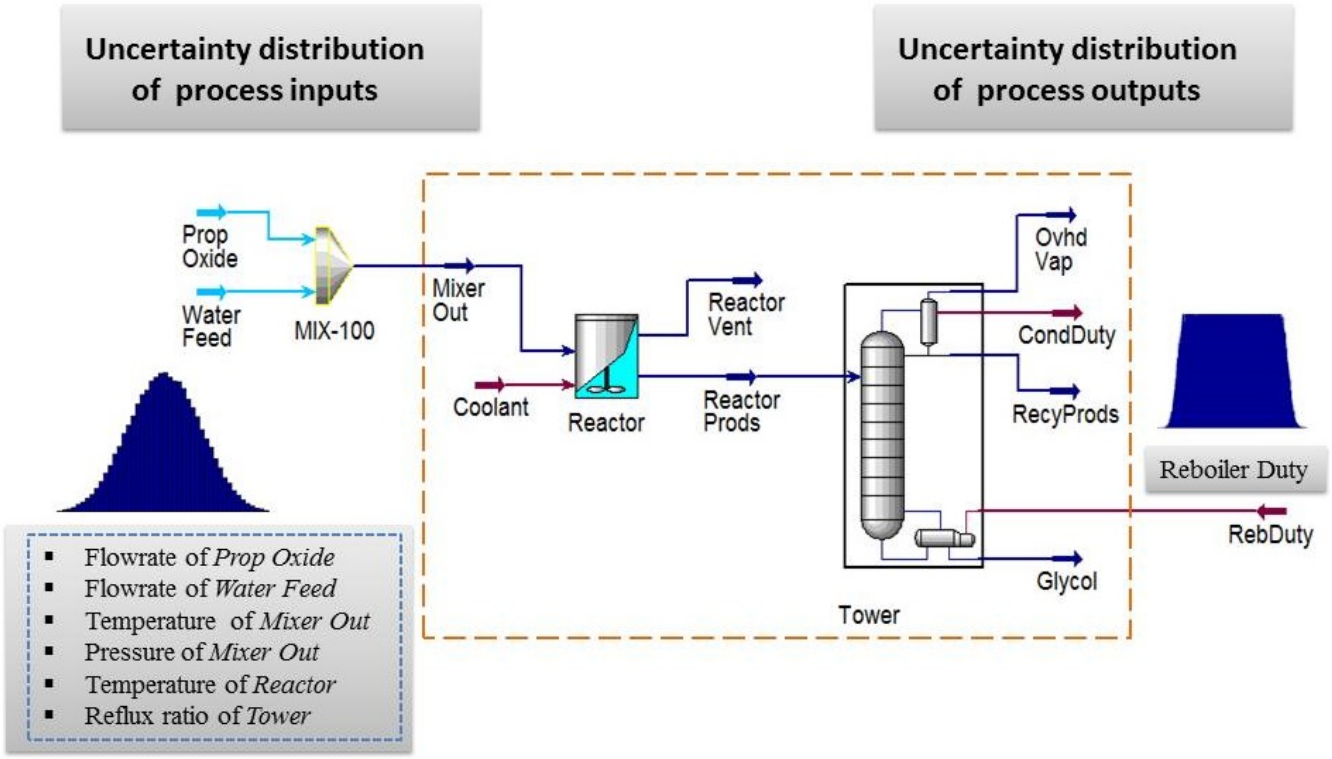

Fig. 3. Propylene glycol (PG) production process (Example 2).

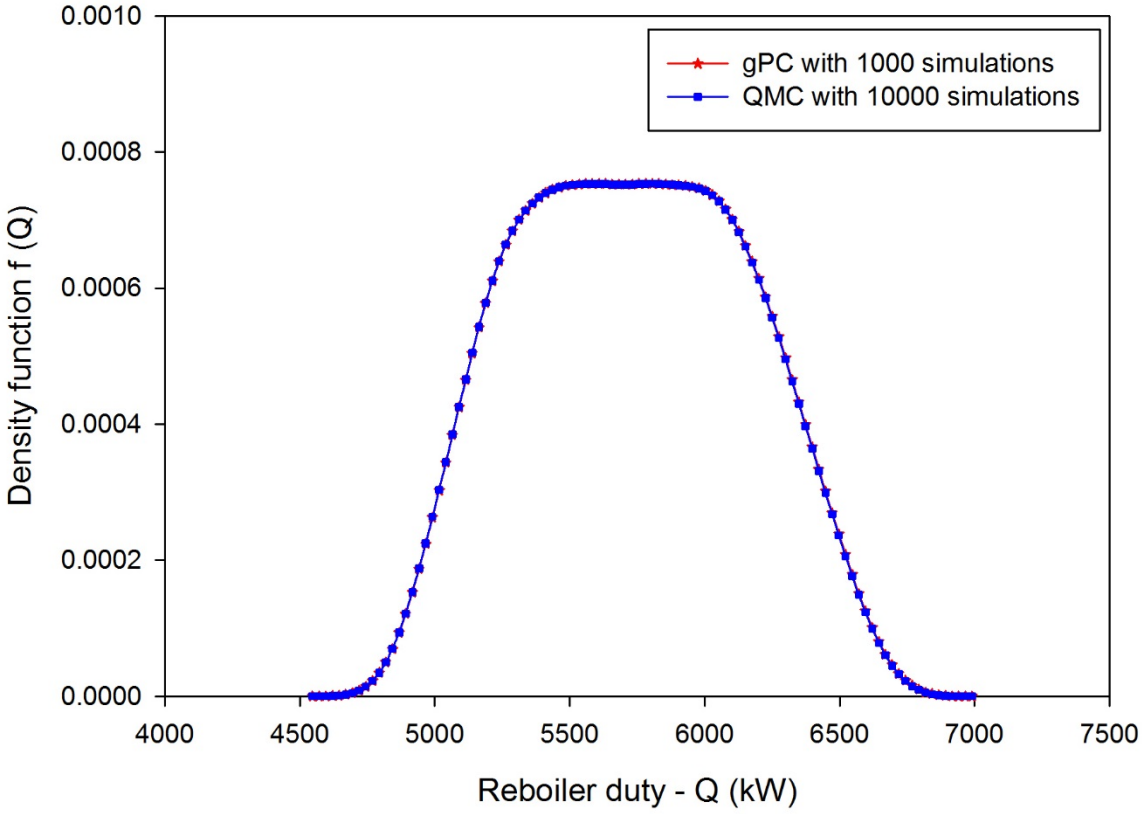

557

558

559 **Fig. 4.** Density distributions of the reboiler duty in the PG production process with 6 uniform random

560 inputs (Example 2).

561

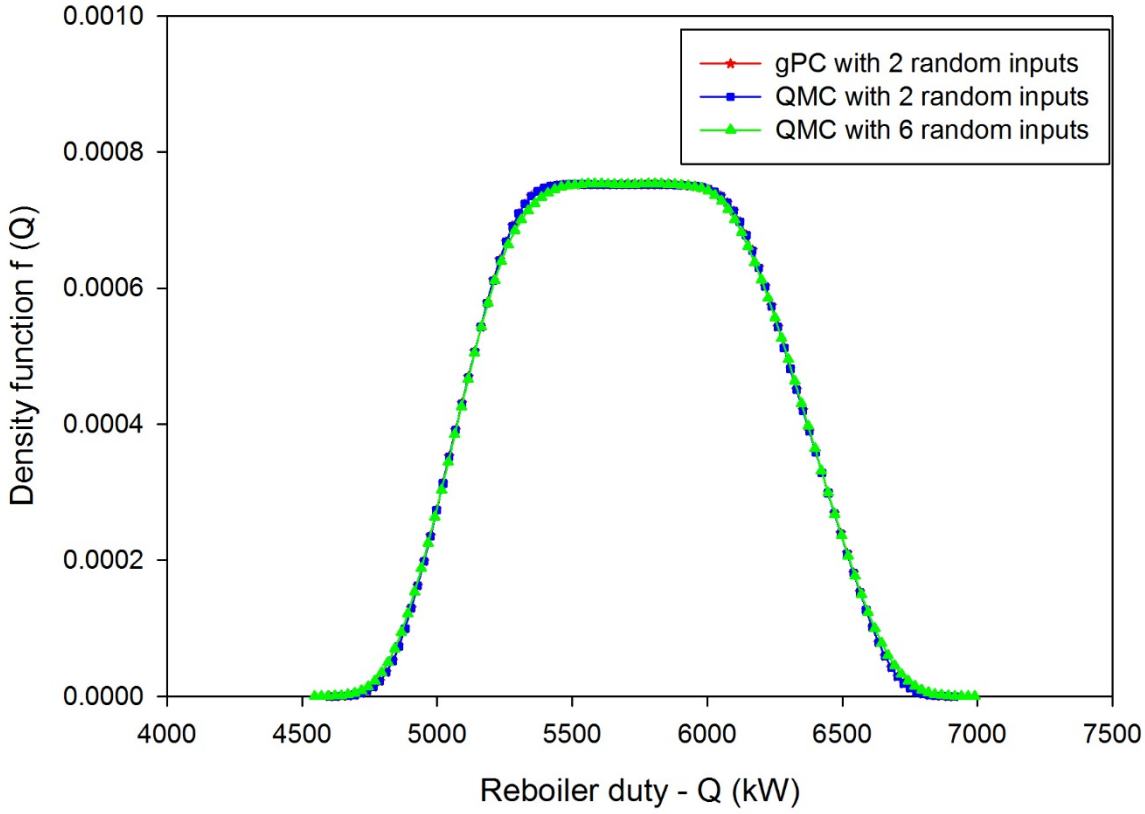

Fig. 5. Density distributions of the reboiler duty in the PG production process with 6 and 2 uniform random inputs (Example 2).

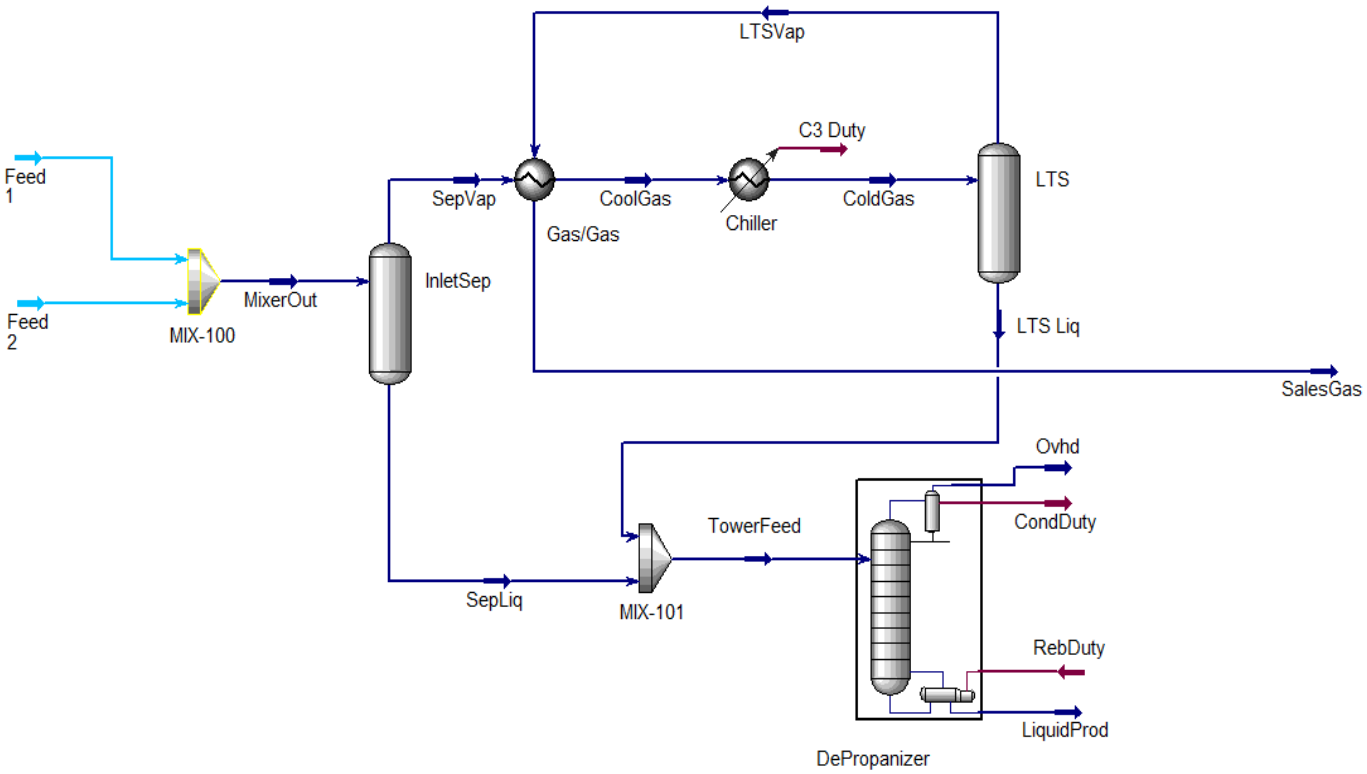

575

576 **Fig. 6.** Lean dry gas processing plant (Example 3).

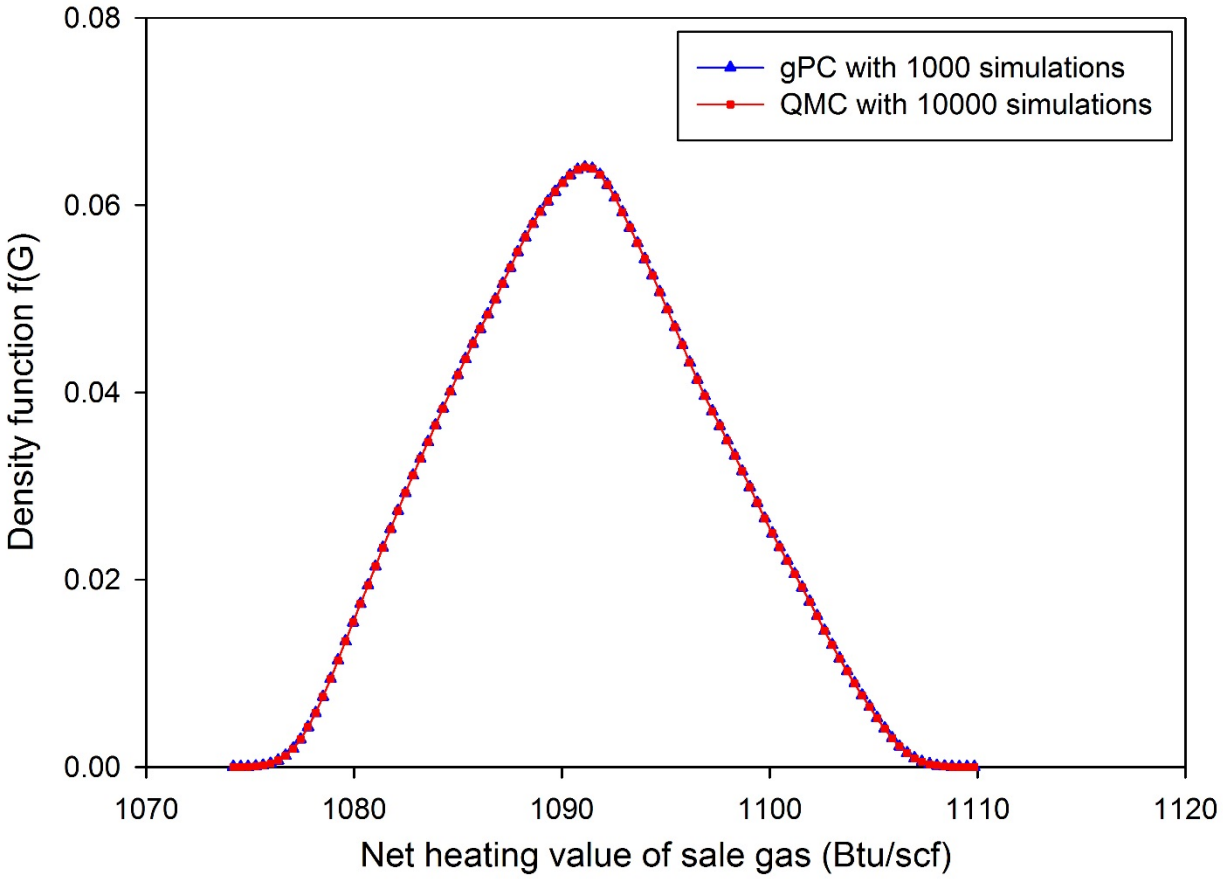

577

578

579 **Fig. 7.** Density distributions of the net heating value of sale gas in the lean dry gas production process with

580 6 uniform random inputs (Example 3).

581

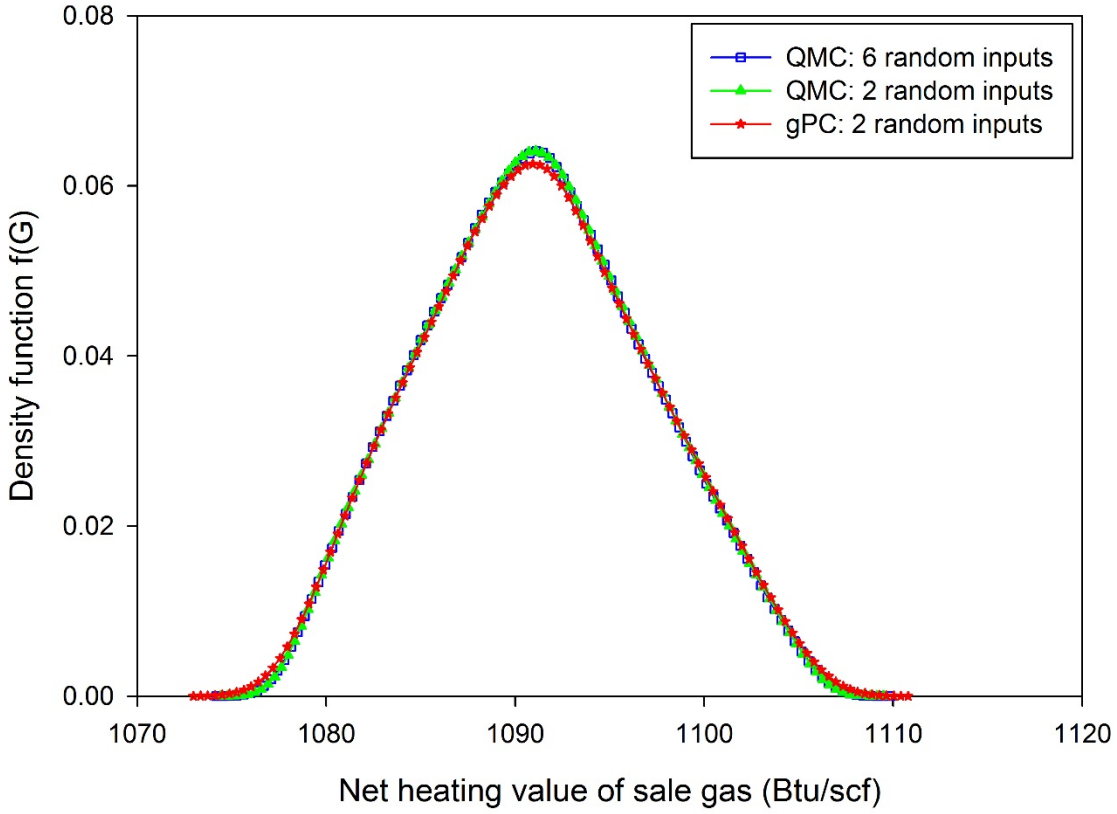

582

583

584 **Fig. 8.** Density distributions of the net heating value of sale gas in the lean dry gas production process

585 (Example 3) with 6 and 2 uniform random inputs.

586

587

588

589

590

591

592

593

594

List of Tables

Table 1. Sensitivity indices of the compressive gPC/standard gPC/QMC methods for Example 1 (Ishigami function) for different sizes of the experimental design set.

Table 2. Simulation parameters and computational time profiles for obtaining the statistical characteristics of the compressive gPC//QMC methods for Examples 2 and 3 (case of 6 random inputs).

Table 3. Sobol′ sensitivity indices from the surrogated gPC model for Examples 2 and 3.

Table 1. Sensitivity indices of the compressive gPC/standard gPC/QMC methods for Example 1 (Ishigami function) for different sizes of the experimental design set

Method		**S1**	**S2**	**S3**	**T1**	**T2**	**T3**
True value		**0.31390**	**0.44241**	**0**	**0.55758**	**0.44241**	**0.24368**
Proposed (compressive gPC)	100 samples	0.31360	0.48352	0	0.54590	0.48647	0.20297
	500 samples	0.31399	0.44248	0	0.55769	0.44244	0.24369
	1000 samples	0.31390	0.44241	0	0.55758	0.44241	0.24368
QMC	500 samples	0.35642	0.46549	-0.13610	0.75706	0.30972	0.15349
	2500 samples	0.32222	0.44231	-0.04484	0.58609	0.40711	0.18485
	5000 samples	0.31395	0.43938	-0.02143	0.55543	0.45050	0.25567
Full gPC	125 samples	0.22969	0.59198	0	0.40801	0.59198	0.17831
	1000 samples	0.31402	0.44219	0	0.55781	0.44219	0.24378
	3375 samples	0.31390	0.44241	0	0.55758	0.44241	0.24368

Table 2. Simulation parameters and computational time profiles for obtaining the statistical characteristics of the compressive gPC/ QMC methods for Examples 2 and 3 (case of 6 random inputs).

Method	Example 2				Example 3			
	No. of simulations	**Runtime (sec.)**	**Mean μ_Q**	**Variance D_Q**	**No. of simulations**	**Runtime (sec.)**	**Mean μ_G**	**Variance D_G**
QMC	10000	19607.6	5730.6	172691.9	10000	19693.8	1091.1	35.5
Compressive gPC	1000	1303.2	5730.5	172832.7	1000	1318.8	1091.1	35.4

Table 3. Sobol′ sensitivity indices from the surrogated gPC model for Examples 2 and 3.

	Sobol′ Sensitivity Indices (S_i, T_i)							
Example 2	**S1**	**S2**	**S3**	**S4**	**S5**	**S6**	**T1**	**T2**
	0.0104	0.8532	1.802e-09	3.687e-09	0.0096	0.1260	0.0105	0.8539
	T_3	**T_4**	**T_5**	**T_6**				
	6.039e-07	4.906e-07	0.0097	0.1267				
Example 3	**S_1**	**S_2**	**S_3**	**S_4**	**S_5**	**S_6**	**T_1**	**T_2**
	4.564e-04	4.557e-04	0.0039	0.5521	0.4429	0	4.57e-4	4.57e-4
	T_3	**T_4**	**T_5**	**T_6**				
	0.039	0.5523	0.4431	4.369e-12				